Manuscript submitted to: Volume 2, Issue 2, 131-152.

AIMS Biophysics DOI: 10.3934/biophy.2015.2.131

Received date 16 February 2015, Accepted date 04 May 2015, Published date 13 May 2015

Research article

Structure of the cystic fibrosis transmembrane conductance regulator in the inward-facing conformation revealed by single particle electron microscopy

Ateeq Al-Zahrani [1,2], Natasha Cant [1], Vassilis Kargas [1,3], Tracy Rimington [1], Luba Aleksandrov [4], John R. Riordan [4], and Robert C. Ford [1,*]

[1] Faculty of Life Sciences, The University of Manchester, Manchester M13 9PT, UK
[2] University College in Qunfudah, The University of Umm-Alqura, Kingdom of Saudi Arabia
[3] Bioinformatics Institute, 30 Biopolis Street, #07-01 Matrix, 138671 Singapore
[4] Department of Biochemsitry and Biophysics, University of North Carolina, Chapel Hill, 6107 Thurston-Bowles, Campus Box 7248, Chapel Hill, NC 27599, USA

*** Correspondence:** Email: robert.ford@manchester.ac.uk.

Abstract: The most common inherited disease in European populations is cystic fibrosis. Mutations in the gene lead to loss of function of the cystic fibrosis transmembrane conductance regulator protein (CFTR). CFTR is a member of the ATP-binding cassette family of membrane proteins that mostly act as active transporters using ATP to move substances across membranes. These proteins undergo large conformational changes during the transport cycle, consistent with an inward-facing to outward-facing translocation mechanism that was originally proposed by Jardetzky. CFTR is the only member of this family of proteins that functions as an ion channel, and in this case ATP and phosphorylation of a regulatory domain controls the opening of the channel. In this article we describe the inward-facing conformation of the protein and show it can be modulated by the presence of a purified recombinant NHERF1-PDZ1 domain that binds with high affinity to the CFTR C-terminal PDZ motif *(-QDTRL*). ATP hydrolysis activity of CFTR can also be modulated by glutathione, which we postulate may bind to the inward-facing conformation of the protein. A homology model for CFTR, based on a mitochondrial ABC transporter of glutathione in the inward-facing configuration has been generated. The map and the model are discussed with respect to the biology of the channel and the specific relationship between glutathione levels in the cell and CFTR. Finally, disease-causing mutations are mapped within the model and discussed in terms of their likely physiological effects.

Keywords: cystic fibrosis; CFTR; electron microscopy; ABCC7

1. Introduction

Cystic fibrosis is an inherited disease that arises due to defects in the cystic fibrosis transmembrane conductance regulator (CFTR) [1]. This membrane protein functions as an ATP-regulated anion channel although it is also a member of the ATP-binding cassette transporter family [2]. Despite the *cftr* gene being identified and sequenced several decades ago [3], work on the purified protein has lagged behind. Loss of CFTR activity in cystic fibrosis sufferers results in many detrimental effects, the most serious being the production of highly viscous mucus [4,5,6] leading to chronic lung infections. By far the most common CF-causing mutation is the deletion of phenylalanine at position 508 (F508del) in the CFTR protein that is thought to lead to misfolding or its destabilization and to cause its degradation by the cell's quality control machinery [7–10]. It is thought that the mutation extenuates the intrinsic instability of the wild-type CFTR protein, a significant proportion of which is also degraded before reaching the plasma membrane [8,9,10]. These properties have hampered the purification and biochemical characterization of the wild-type protein, whilst even obtaining detectable levels of the F508del version has been challenging. These problems need to be overcome in order to understand the role of CFTR in the progression of the disease and to develop new therapeutic strategies to address the basic defect.

Murine and human CFTR orthologs have been shown to be expressed at moderate levels in the yeast *S. cerevisiae*, with about 80 μg purified protein obtained per litre of cell culture [11,12,13]. Yeast may be a useful system for CFTR expression as it can be grown rapidly at temperatures around 20 ℃ where even the F508del version of CFTR is known to be comparatively stable. At these temperatures, mammalian CFTR will also have much reduced channel activity, which may be crucial because unregulated anion flux could be toxic to the host cell at the high CFTR expression levels needed for purification purposes. Unlike bacterial expression systems, yeast is able to carry out most of the post-translational modifications of CFTR, and it carries out a more limited (core) glycosylation that may be advantageous in terms of monodispersity. Purification of CFTR from yeast membranes has previously been described using the lyso-phosphatidyl glycerol detergent LPG14. With this negatively-charged detergent, CFTR can be efficiently extracted from the membranes and purified to homogeneity [11–14]. Although lyso-lipid detergents have been shown to be very effective for some membrane proteins [15], for other proteins they seem to cause significant destabilization and loss of biochemical activity [16]. Moreover charged and zwitterionic detergents are often considered to be relatively harsh compared to uncharged detergents [17,18]. The detergent-solubilisation of membrane proteins often causes their destabilization [19], hence there will be a delicate balance between the efficiency of extraction of a given membrane protein and retention of its biochemical activity. For example, sodium dodecyl sulphate could be employed to purify most membrane proteins, but the resultant products would probably be biochemically inactive. In line with other studies, LPG14-purified CFTR has low ATPase activity. Ion flux has been reported with such LPG-solubilised preparations [12,14] (after CFTR reconstitution with lipid and removal of the

detergent). However quantitation of this activity is difficult. Even a very small percentage of the CFTR molecules retaining a native configuration could account for the measured flux of ions, and similarly, single channel measurements arise from just one active CFTR molecule.

The C-terminal region of CFTR consists of hydrophilic and charged amino acid residues and with the last four residues (-DTRL^{1480}) representing a well-characterised PDZ-binding motif. The latter is able to bind to NHERF1 and NHERF2 proteins in the cell via their PDZ domains. The main role of the NHERF family is the formation of a multiprotein complexes to regulate the activities of other proteins. Each PDZ domain within NHERF proteins has a length of 80–100 amino acids [20] and regulates protein-protein interactions by binding to short peptides, most often, but not exclusively in the carboxy- terminii of target proteins [21,22]. To date, six PDZ proteins (NHERF1, NHERF2, NHERF3, NHERF4, Shank2 and CAL) have been reported to interact with the C-terminus of CFTR. The first five proteins are proposed to interact with CFTR in the apical membrane of epithelial cells, while separate data suggest that CAL (CFTR-associated ligand) interacts with CFTR in the Golgi [23,24]. A short carboxyl-terminal peptide of CFTR (QDTRL) fused at the C-terminus of NHERF 1 PDZ1 was expressed in BL21 (DE3) *E.coli* cells and its structure was solved [21].

NHERF family proteins have been proposed to regulate CFTR in several ways [25]. The mechanism by which a simple binding to a flexible region is able to regulate the protein is not clear, however. Recent in-vitro studies on interactions between purified CFTR C-terminus peptide and purified CFTR regulatory region imply that phosphorylation may be an important additional factor in this process [26]. Independent of mechanism however, NHERF proteins appear to be a potential therapeutic target for the treatment of CF. For example Guerra and co-workers, [27] found that mouse NHERF1 (but not NHERF2) overexpression increased F508del-CFTR plasma membrane expression and activity in human bronchial epithelial cell. Similarly, Bossard and co-workers [28] reported that F508del-CFTR apical plasma membrane expression and chloride channel activity were restored by human NHERF1 overexpression.

Structural analyses of CFTR have been carried out on isolated soluble domains as well as the full length protein. For the latter, electron cryomicroscopy (cryo-EM) with single particle analysis has been employed [29,30] as well as electron crystallography of two-dimensionally ordered arrays [31]. Whilst the former studies were carried out on dimeric particles isolated by size exclusion chromatography, the two dimensional crystals were formed by monomeric CFTR particles organised in a double layered arrangement. In both cases, the structural data for CFTR was interpreted as showing an outward-facing configuration of the protein, similar to some ABC transporter structures [32,33]. However, the CFTR outward-facing configuration was detected in the absence of nucleotide. In contrast a recent cryo-EM study of CFTR expressed in HEK cells and then purified in facial ampiphile detergents and with 1mM ATP revealed monomeric CFTR particles [34] and these were interpreted as being in an inward-facing conformation. Hence some plasticity in the tertiary and quaternary structure of CFTR is observed in the detergent micelle and with counter-intuitive behaviour in the presence of ATP.

2. Materials and Methods

2.1. Expression and Purification of proteins

A GST-tag vector (pGEX-2TJL1) containing NHERF1 PDZ $1^{(+)}$ (residues (after thrombin cleavage) GSSRM-11–94 and the carboxyl-terminal extension N95DSLL99 that corresponds to residues 409–413 of human β_2AR) was expressed in BL21 (DE3) *E.coli* cells. 0.1 mM IPTG was used for induction. Sonication, wash and elution buffers were respectively, (140 mM NaCl, 10 mM Na_2HPO_4, 1.8 mM KH_2PO_4, 0.1% TritonX-100, 100mg/ml Lysozyme), (140 mM NaCl, 10 mM Na_2HPO_4, 1.8 mM KH_2PO_4), (33 mM Glutathione in 50 mM Tris-HCl pH 8). Glutathione resin (Clontech) was used. After collection of unbound material and a wash step, the protein was eluted by cleavage from its GST-tag by thrombin in 50 mM Tris-HCl pH 7.7, 300 mM Potassium Acetate, 7 mM Magnesium Acetate, 10% (v/v) Glycerol (at 4 ℃ overnight). After purification, the protein was concentrated using Centricon Centrifugal Filter Units (Millipore) by collecting the filtrate passing through a 50 kDa cut-off filter, and then concentrating this with a 3 kDa cut-off filter. Expression and purification levels were determined by SDS-PAGE. Gel filtration using a Superdex 200 column was used as a polishing step with 100 mM NaCl, 50 mM Tris pH 7.5, 0.01% Sodium Azide (NaN_3), 1 mM 2-Mercaptoethanol, 1 mM EDTA running buffer. Mass and purity were confirmed by SDS-PAGE and MALDI-TOF [35]. Various full-length CFTR orthologs were expressed in yeast and purified as described in [36]. CFTR samples were also expressed and purified in lyso-phosphatidyl glycerol (LPG, 0.05% w/v) as described in [11,36]. For reconstitution with lipid and cholesterol, procedures were as described in [36]. Samples of the reconstituted CFTR samples were also assessed by negative stain electron microscopy. Full-length human CFTR was also expressed in BHK cells and purified in dodecyl maltoside (DDM) as described in [29].

2.2. ATPase activity

The CFTR-specific ATPase activity was determined using a Chifflet assay in a 96-well plate format [37,38,39]. Any residual activity of extraneous P-, F- and V-type ATPases was minimised by adding a cocktail of 10 μM Sch28080, 10mM NaSCN and 25 μM oligomycin [39] which have been shown to have no effect on CFTR gating [40].

2.3. CFTR interaction assay

Full-length CFTR was bound to Talon metal affinity chromatography (IMAC) resin equilibrated with 15 μL of buffer (150 mM NaCl, 40 mM Tris pH 7.5, 0.01% sodium azide (NaN3), 0.05% n-dodecyl- β- D- maltoside (DDM), 5 mM 2-mercaptoethanol). For LPG-purified CFTR the buffer was 50 mM NaCl, 20 mM HEPES pH 7.5, 0.05% LPG. After washing to remove unbound CFTR, purified NHERF1 PDZ1 was added to the resin (15 μL) and incubated for 2 hr with gentle rotation. The resin was washed 6 times with 15 μL of buffer (DDM or LPG containing buffers as above). Elution was with two washes with the same buffer plus 400 mM imidazol. Residual protein remaining bound to the beads, if any, was detected with a 1% w/v SDS final wash step. All steps

were performed at 4 ℃. SDS-PAGE gels were Silver-stained (Thermo, FERMENTAS). For reconstituted CFTR the same procedure was carried out, but with centrifugation as above to separate bound from unbound NHERF1 PDZ1.

2.4. Single Particle Analysis (SPA) Electron Microscopy

Procedures followed those described in [30]. Images of negatively-stained samples were recorded on a FEI Biotwin transmission electron microscope at different defocus values in the range 0.1 μm to 0.5 μm and under low dose mode with 1 second exposures and with 100 kV accelaration voltage. A live FFT from a nearby area of the grid was used to check for astigmatism drift and defocus. SPA was performed using the EMAN2 software package [41]. Homogenous particles that were not overlapping or in close contact with other particles were interactively selected using a box size of (48 × 48 pixel) and Å/pixel of 5.2 (negatively stained samples). Sets of reference-free class averages were generated representing different characteristic views or orientations of single particles. 20 to 30 characteristic views of the classes representing top, side and partial views were selected and used for the reconstruction of a preliminary 3D model with C2 symmetry applied on the basis of previously published studies [42,43]. Further rounds of refinement where the symmetry was relaxed were included for monomeric CFTR particles. The relative orientations of the characteristic views were determined using a Fourier common-lines routine, and the resulting averages were combined to generate the preliminary 3D model. Initial 3D structures were refined subsequently using 6 rounds of iterative projection matching with each refinement evaluated by examining the convergence by comparison of the Fourier shell correlation (FSC) of the 3D model generated with the previous iteration. The final 3D structures were low pass Gaussian-filtered to the resolution indicated by the shell corresponding to a correlation coefficient of 0.143 [44] in the FSC plot calculated between two structures, each calculated from half the dataset (often termed the even-odd resolution test).

2.5. Molecular modelling

Sequence alignment was performed with CLUSTALW for each half of CFTR against Atm1 [45]. Modifications of the PDB file were performed utilizing the PDB cleaner routine[46]. The alignment was then utilized by the Modeller 9.11 program [47] for the generation of multiple structural models and the best was selected [48]. Energy minimization was carried out using MMTK running within the Chimera software suite using 1000 steps of steepest descent, step size 0.002 nm, followed by 10 steps of conjugate gradient minimization (step size 0.002 nm) with no atoms fixed, hydrogen atoms included and charged residues assigned [49].

3. Results

3.1. CFTR purification.

Full-length CFTR expressed in *S. cerevisiae* was purified in detergent DDM or LPG. Examples of the degree of purity achieved with these procedures are shown in Supplementary Figures 1 and 2.

In general, purity is higher with the LPG detergent, although activity and thermal stability are lower (see below). The main contaminating protein in the presence of DDM was the yeast large ribosomal subunit L3, however this does not have any ATPase activity nor does it interfere with the thermal stability assay (Cant, N. 2014, University of Manchester PhD Thesis).

3.2. CFTR reconstitution

Full-length CFTR expressed in *S. cerevisiae* and purified in DDM was reconstituted overnight at 4 ℃ with *E.coli* lipids containing 20% cholesterol (w/w) [36,39]. Reconstitution was checked by SDS-PAGE and EM (Figure 1). The time allowed for reconstitution was crucial. An overnight (14 hr) incubation with the beads resulted in little loss of CFTR (Figure 1A) and electron microscopy showed that the reconstituted material was composed of a mixture of membrane sheets and smaller vesicles (Figure 1B), with no evidence of protein aggregates nor detergent-solubilised single particles [50,51]. However a further 24hr incubation with a fresh batch of adsorbent beads resulted in loss of most of the membranes to the beads (Figure 1A). The treatment of the beads with SDS released the membrane-bound CFTR (Figure 1A), but it migrated as large molecular mass SDS-resistant aggregates.

3.3. ATPase activity of purified and reconstituted CFTR

Incubation of CFTR at 25 ℃ with 2 mM ATP over a standard 60 min period liberated inorganic phosphate due to ATPase activity (Table 1). Reconstitution of CFTR with lipid significantly increased the amount of phosphate (a lipid-only mock reconstitution was employed as control for these experiments). For DDM-purified material, the activity was increased 4.4-fold after reconstitution with lipid. In comparison CFTR purified in LPG had a lower ATPase activity (Table 1) which increased by 3 fold upon reconstitution. CFTR purified in DDM was also incubated with PKA and ATP and subsequently reconstituted. When compared with a mock-treated control or with untreated protein that was directly reconstituted, there were no significant differences in the ATP hydrolysis activity (Table 1). Others have shown stimulation of CFTR ATPase activity after PKA treatment [52]. However, in the yeast expression system, CFTR appears to be already phosphorylated (Supplementary Figure 3, [53]). We also tested some known modulators of CFTR channel activity for effects on the ATPase activity. Neither genistein, nor CFTR inhibitor-172 showed any significant effect on the ATPase activity (Table 1). However the presence of 10 mM glutathione resulted in a significant inhibition of the ATPase activity of the purified and reconstituted CFTR protein as reported previously [14,54].

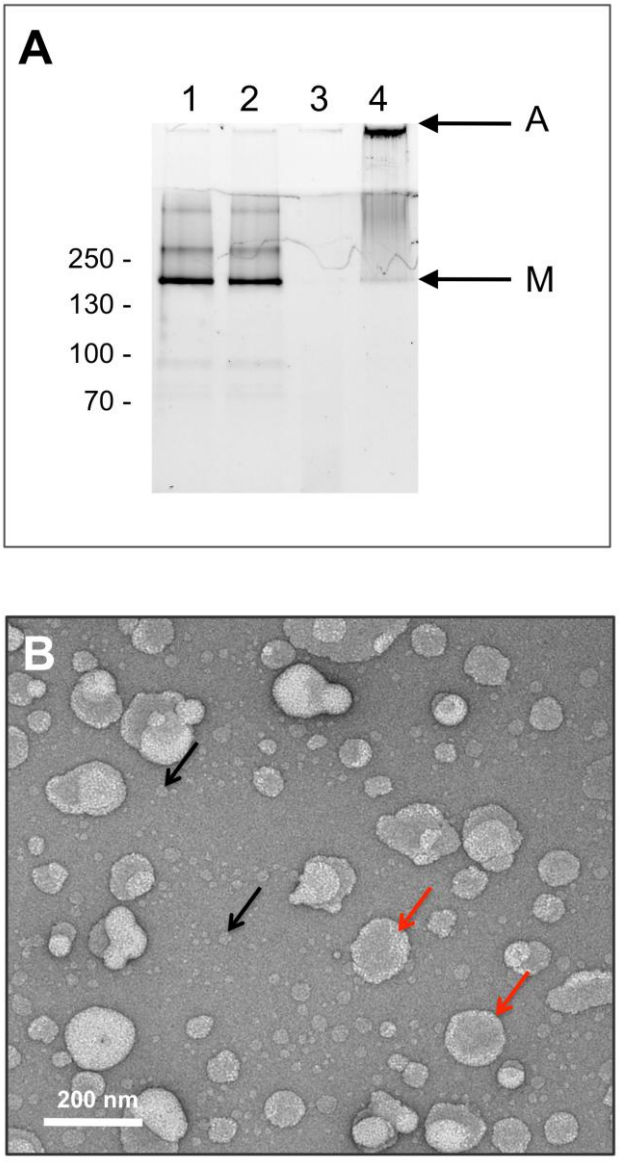

Figure 1. A. SDS-PAGE of CFTR reconstituted by detergent removal by Biobeads. DDM-purified CFTR was mixed with lipids (lane 1) and then incubated with Biobeads overnight (lane 2). A proportion of the material was transferred to fresh Biobeads and incubated for a further 24 hr (lane 3). Material associated with the Biobeads was denatured and released by the addition of SDS (lane 4). CFTR protein migrated as a monomer band (M), or as an SDS-resistant CFTR aggregate which was in the Biobead-bound material. B. Electron micrograph of negatively-stained membranes after the 1st Biobead addition (corresponding to lane 2 in Figure A). A mixture of larger liposomes of 150 nm diameter (red arrows) and smaller lipid patches around 20–30 nm (black arrows) were observed.

Table 1. Summary of ATPase activity experiments for CFTR. In each case, phosphate release was measured over 60 minutes using the Chifflet assay. Each condition was repeated 3 times and the mean and standard deviation are given. Three different batches of DDM-purified CFTR were employed, the second batch was employed in the phosphorylation experiments (5, 6), whilst the third batch was employed in the inhibitor experiments (rows 7–10). There were no significant differences in the ATPase activities of the 3 batches after reconstitution (rows 1,5,7).

CFTR Sample/ Experiment	nmol ATP hydrolysed/min/mg CFTR integrated over 60 min (±SD)	% of control (experiment 1)
1. DDM purified/reconstituted	13.2 ±3.0	100
2. DDM purified	3.0 ±0.3	23
3. LPG purified/reconstituted	1.3 ±0.4	10
4. LPG purified	0.4 ±0.1	3
5. As 1 but mock PKA +ATP treatment	13.1 ±2.9	99
6. As 5 after PKA +ATP treatment	14.0 ±2.8	106
7. As 1 but mock inhibitor treatment	13.6 ±0.4	103
8. As 7 + 10μM inh-172	13.4 ±0.5	102
9. As 7 + 0.1mM genistein	13.5 ±0.3	102
10. As 7 + GSH 10mM	6.6 ±2.5	50

3.4. Kinetics of ATPase activity

The ATP concentration-dependence of the phosphate release was measured for the reconstituted protein (Figure 2A) and it showed a saturable behaviour with a Km of 0.14mM ATP and a maximal phosphate release of 13.4 nmol/min/mg CFTR (averaged over the 1hr time period). However the time-course of phosphate release revealed a rapid tail-off at 25 ℃, showing little or no further phosphate liberation after the standard incubation time (60 min) as shown in Figure 2B. The V_{max} based on the rate of phosphate liberation over the first 5 mins was about 50–90 nmol P_i/min/mg CFTR for different batches of protein, equivalent to a k_{cat} of 0.25 s^{-1}. Gating measurements for BHK

cell-expressed chicken CFTR at this temperature are consistent with a mean interburst interval of about 4–6 seconds [55]. We also examined the concentration dependence of glutathione inhibition at 2mM ATP, with an almost complete inhibition of activity at 20mM glutathione (Figure 2C).

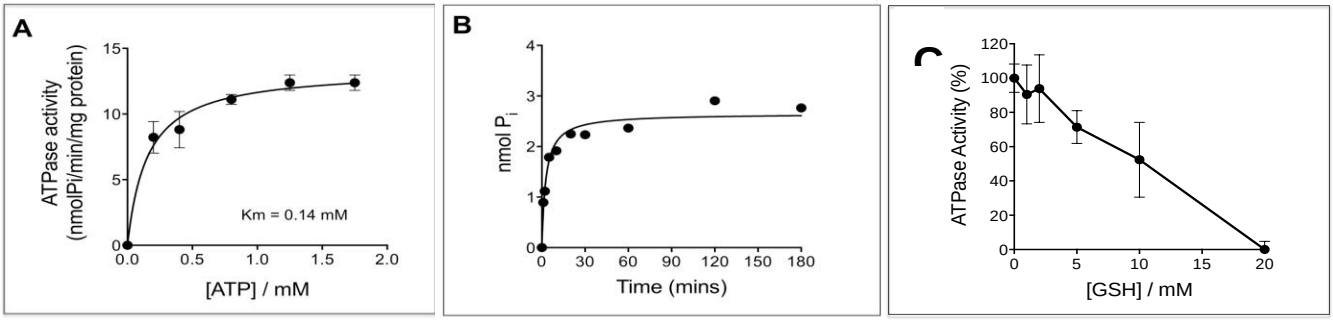

Figure 2. CFTR—dependent phosphate release as a function of: ATP concentration (A), time (B), and glutathione concentration (C). A. Phosphate release at 25 ℃ was fitted with the Michaelis-Menten relationship using non-linear regression in GraphPad Prism software. Error bars show the mean ± S.D. of triplicate experiments. B. The kinetics of phosphate release shows that CFTR ATPase activity is lost within 2 hours at 25 ℃ and already shows a significant run-down after 20 min. C. Glutathione inhibits the activity, with 50% inhibition at 10mM glutathione (GSH).

3.5. CFTR thermal stability

We tested whether the rapid run-down of ATPase activity of CFTR was due to thermal instability of the protein. Figure 3A shows the ATPase activity of CFTR after a 5 min pre-incubation at various temperatures (average of two measurements). Approximately 35% of the activity was lost in a 5 min pre-incubation at 25 ℃ (the ATPase assay temperature), which is consistent with the kinetics shown in Figure 2B. At physiological temperatures (40 ℃), about 50% of the ATPase activity is lost within 5 min. Studies of the isolated CFTR NBD1 thermal stability by differential scanning calorimetry suggested that very limited unfolding may occur at physiological temperatures [16], although the domain is significantly unstable in the presence of detergent at around 40 ℃. The thermal stability of NBD2 (which is probably more important than NBD1 for ATPase activity) remains unknown at present. We tested the global unfolding of DDM-purified CFTR at increasing temperatures using two assays: In the first assay [56] fluorophore-binding was employed to detect a gradual exposure of buried Cysteine residues at increasing temperatures. This showed a maximum signal at about 65 ℃ and a midpoint for the transition at about 50 ℃ (Figure 3A). In this assay, some unfolding of purified chicken CFTR is implied even at physiological temperatures as detected by exposure of previously inaccessible Cysteine residues. This is in approximate agreement with the temperature-dependent loss of ATPase activity of reconstituted CFTR (Figure 3A), although for the fluorophore-binding measurements, the presence of detergent (DDM) may cause additional destabilization [16]. A second assay was employed that detects the

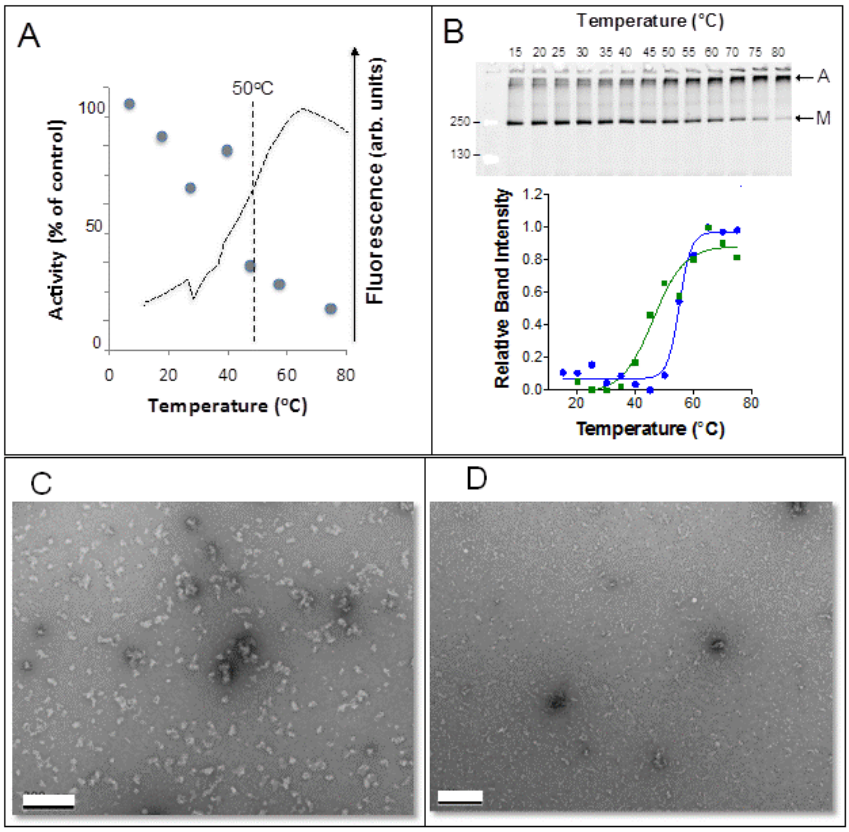

Figure 3. A. ATPase activity of CFTR after incubation for 5 min at various temperatures (circles). Data shown are the average of two experiments. The dashed curve shows the fluorescence of a Cys-reactive fluorophore, CPM incubated with CFTR and as a function of temperature. The fluorescence shows a transition centred about 50 ℃ indicating protein unfolding and exposure of Cys residues to the fluorophore. B. Detection of CFTR unfolding by the formation of SDS-resistant species (A) and disappearance of the monomeric CFTR band (M). The lower graph shows quantitation of the relative intensity of the "A" band as a function of temperature for DDM-purified CFTR (circles) compared to CFTR in the presence of a harsher anionic detergent LPG(squares). Panels C and D show negatively-stained specimens of CFTR before (C) and after (D) heating to 90 ℃. Scale bars represent 100 nm.

formation of SDS-resistant aggregates at high temperatures [57,58] (Figure 3B). Formation of such aggregates is particularly associated with membrane proteins and probably relates to exposure of their transmembrane hydrophobic residues after denaturation. When analysed in this way, CFTR shows a strong cooperative effect that has a midpoint temperature of about 55 ℃ for the DDM-purified protein. A harsher detergent such as LPG appears to broaden the unfolding transition and shifts it to lower temperature, consistent with the idea that this method is detecting the stability of the protein (Figure 3B). Negative stain electron microscopy of DDM-purified CFTR before and after thermal denaturation is displayed in Figure 3C and D. Denaturation does not cause aggregation of the

protein, but rather a change in the size and staining of the particles, presumably due to the complete unfolding of the polypeptide chain and loss of tertiary structure. We concluded from these various studies that CFTR expressed in yeast was folded and active after purification in DDM, with much less activity and stability when isolated in LPG.

3.6. NHERF1-PDZ1/CFTR Interactions

Co-expression of the CFTR C-terminal peptide (terminal 42 residues) and the NHERF1-PDZ1 domain was carried out in *E.coli* and the peptide/protein complex was subsequently affinity-purified using an N-terminal hexa-Histidine tag on the peptide (Supplementary Figure 4A, [59]). The NHERF1-PDZ1 domain alone was also expressed in *E.coli* and the protein was subsequently affinity-purified using an N-terminal GST tag. Following GST tag cleavage, the NHERF1-PDZ1 domain was separated and then concentrated using 50 kDa and 3 kDa cutoff microconcentration devices respectively (Supplementary Figure 4B, [59]). Individual components and the peptide-NHERF1-PDZ1 domain complex were all characterised by mass spectrometry (Supplementary Figure 5). Some evidence of post-translational or post-purification modification was apparent. The

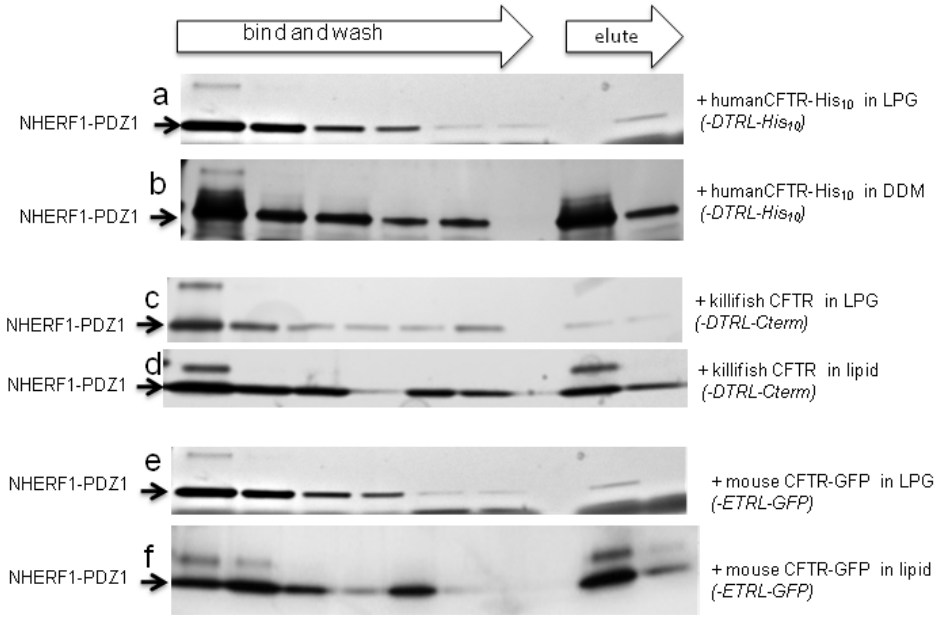

Figure 4. Interaction of NHERF1-PDZ1 domain with full-length CFTR as detected by SDS-PAGE and silver staining of the domain band. In the presence of LPG detergent, a rapid wash-out is observed (a) but in DDM wash-out is slower and significant levels of the domain remain bound (b). A similar effect is observed for a LPG-purified CFTR with a wild-type C-terminus (c). In this case, reconstitution was found to restore binding of NHERF1-PDZ1 (d). Similar behaviour was observed even when the PDZ-binding motif was internalised by a GFP tag (e, f).

purified NHERF1-PDZ1 domain alone was found to associate as a dimer of 20 kDa mass (Supplementary Figure 6), as detected by size-exclusion chromatography—multi-angle light scattering (SEC-MALS) and as predicted by structural studies of the domain which showed homodimers associating by mutual binding of their C-terminal residues [60]. Since co-expression of untagged NHERF1-PDZ1 domain with the His-tagged C-terminal peptide in *E.coli* allowed co-purification of both components, we concluded that NHERF1-PDZ1 interacts more strongly with the 42-mer C-terminal peptide of the human CFTR sequence than with its own C-terminus [59].

Theoretical calculations using the PISA server [61] also predict that the NHERF1-PDZ1-bound –DTRL C-terminal peptide will associate more strongly, with a dissociation free energy of +4.3 kcal/mol versus −5.7 kcal/mol for the –DEQL sequence present in the NHERF1-PDZ1 homodimer [60,62,63].

We further studied the interaction of NHERF1-PDZ1 with the full-length CFTR protein, with the latter immobilised on Ni-NTA resin which was then incubated with purified NHERF1-PDZ1 domain (Figure 4). NHERF1-PDZ1 domain was found to interact with the full-length human CFTR protein expressed in BHK cells and purified in DDM, implying that the C-terminus is accessible, despite it being internalised by a poly-His purification tag (Figure 4b). The interaction with NHERF1-PDZ1 was noticeably less with full-length CFTR purified in LPG as indicated by a faster bleed out of the protein during wash steps and a much lesser degree of finally eluted material (Figure 4 a,c,e). After removal of LPG detergent using polystyrene beads and reconstitution of the CFTR protein with lipid, the strong interaction of CFTR with NHERF1-PDZ1 was restored (Figure 4 d,f), implying that LPG in some way interferes with the interaction.

3.7. Structure of CFTR with NHERF1-PDZ1

Human CFTR expressed in BHK cells has previously been purified and studied by single particle electron microscopy. Dimeric complexes of the protein were isolated by size-exclusion chromatography and were interpreted as being in an outward-facing configuration [64] in the presence of both DDM and LPG detergents. We incubated the same protein in the presence of DDM and NHERF1-PDZ1 and carried out single particle analysis after negative-staining of the resultant complexes. Dimeric complexes were observed as before (Supplementary Figure 7), but after addition of the NHERF1-PDZ1 domain there appeared to be a much greater separation of density in a region assigned to the cytoplasmic NBDs (Figure 5), indicative of a conformational change for the CFTR protein.

We also studied CFTR expressed in yeast cells and subsequently purified in DDM or LPG detergents. In this case, monomeric CFTR particles were predominant in the presence of DDM (Figure 6). As before, the addition of NHERF1-PDZ1 induced a wider separation of the NBDs interpreted as a switch to an inward-facing conformation (Figure 6b). Similar studies were carried out with CFTR in the presence of LPG and NHERF1-PDZ1 (Figure 7), but in this case, the addition of the NHERF1-PDZ1 domain led to the formation of linear oligomeric aggregates of CFTR that were not amenable to single particle analysis because of their variable length and overall curvature (Figure 7, right hand panel). Nevertheless, the stark change in the association behavior of CFTR after

addition of NHERF1-PDZ1 implied a major influence of the domain on the conformation of the full-length protein.

4. Discussion

Purified and reconstituted CFTR at 25 ℃ hydrolyses ATP about once every 4 seconds. This closely mirrors the frequency of channel opening and closing cycles for the chicken ortholog of CFTR at this temperature [55] and supports a model linking ATP binding with channel opening and ATP hydrolysis with closure [65]. CFTR channel blockers $CFTR_{inh}$-172 and genistein did not affect the ATPase activity (Table 1) suggesting that these compounds simply block the channel rather than affecting the open probability via allosteric effects on the ATPase activity [66,67]. An effect of $CFTR_{inh}$-172 on ATPase activity human CFTR purified in other detergents has been reported [52,68] suggesting that further comparative studies on this compound are merited. $CFTR_{inh}$-172 is able to significantly inhibit chicken CFTR-associated chloride currents in kidney proximal tubules [69], hence the differing effects of $CFTR_{inh}$-172 on chicken and human CFTR are unlikely to be due to evolutionary divergence.

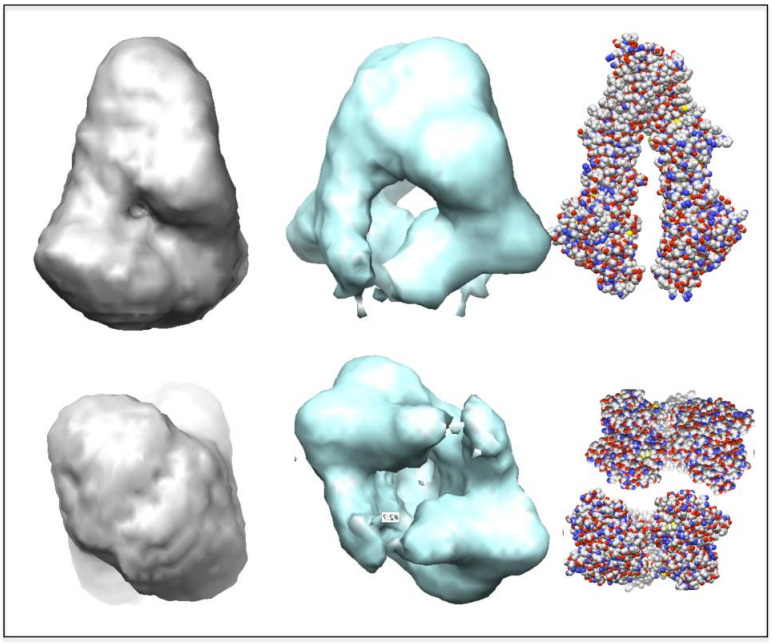

Figure 5. Coulomb density maps derived from negatively-stained dimeric CFTR particles isolated in the detergent DDM (grey, light blue surfaces). The top row shows side-views of the particles, whilst the bottom row shows the same particles viewed from the bottom (assumed cytoplasmic facing region) after rotation around the x axis by 90^{o}. For comparison, the X-ray structure of P-glycoprotein (PDB 3G5U) is shown on the right using a space-filling model. Compared to control (grey surface), the addition of the NHERF1-PDZ1 domain caused a change in conformation with a greater separation of domains at the bottom of the complex (blue surface).

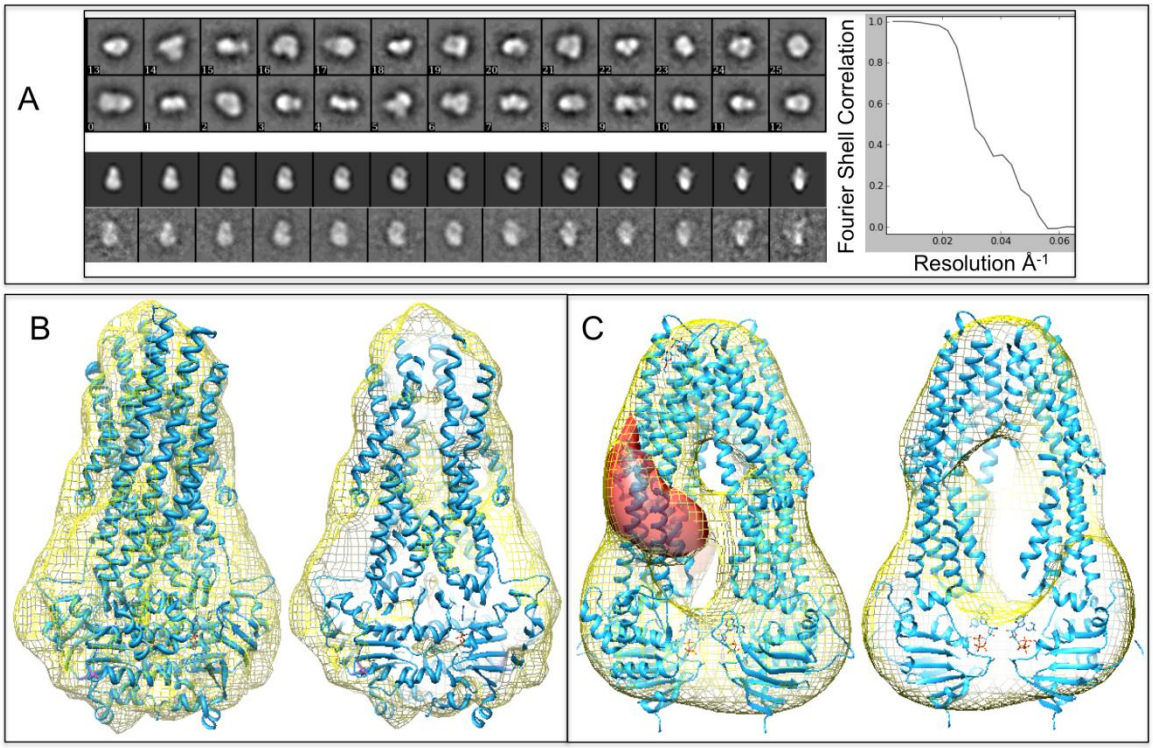

Figure 6. A: Top panel shows a classification of monomeric particles for negatively stained CFTR expressed in yeast and purified in DDM. The lower panel shows re-projections of the final 3D structure and the corresponding raw particle averages. On the right is shown an estimate of the resolution of the final unsymmetrised map calculated by splitting the dataset into two and then calculating the Fourier shell correlation between each half dataset's 3D map. B: Two views of the 3D map of CFTR in the absence of NHERF1PDZ1 domain (yellow mesh defines the expected molecular envelope). Fitted into the map is the bacterial Sav1866 structure (PDB 2HYD) which is in the outward-facing conformation and fits to the CFTR map with little additional density and with a high correlation coefficient. The view on the right shows a central slice through the map. C: Similar two views of the 3D map of CFTR in the presence of the NHERF1PDZ1 domain. A greater separation of the two halves of the molecule is indicated. Fitted into the map is the mitochondrial ABCB10 transporter (PDB 4AYW). The model fits well into the CFTR map except for a lobe of density on one side indicated by the red surface. This may represent some localized density for the regulatory region of CFTR.

The inhibition of CFTR ATPase activity by glutathione is intriguing and is unlikely to be due to redox processes as the CFTR samples already contain 2 mM dithiothreitol. The ABCC family, of which CFTR is a member, contains transporters of glutathione or glutathione-conjugated substrates [70,71]. Glutathione concentrations in the cytoplasm have been reported to be in the range 0.5–10 mM [72], hence from the data in Figure 2C it would imply that this component of redox homeostasis will have an impact on CFTR ATPase activity *in-vivo*. High cytoplasmic concentrations

of glutathione and inhibition of ATP hydrolysis might prolong CFTR channel opening if its effect is simply on catalysis at the active site in the NBDs. This would lead to greater chloride (and glutathione diffusion) into the extracellular fluid [73] and provide a feedback mechanism to regulate intracellular glutathione concentrations. Interestingly, CF sufferers appear to have low glutathione concentrations in the airway surface liquid layer [74] which may pre-dispose them to oxidative stress during inflammation [75]. Polymorphisms associated with glutathione metabolism act as modifiers of CF severity in patients [76]. In line with the idea of CFTR acting as an important regulator of glutathione levels, CFTR inhibition has recently been shown to reduce intracellular oxidative stress due to cisplatin, an anti-cancer drug [77].

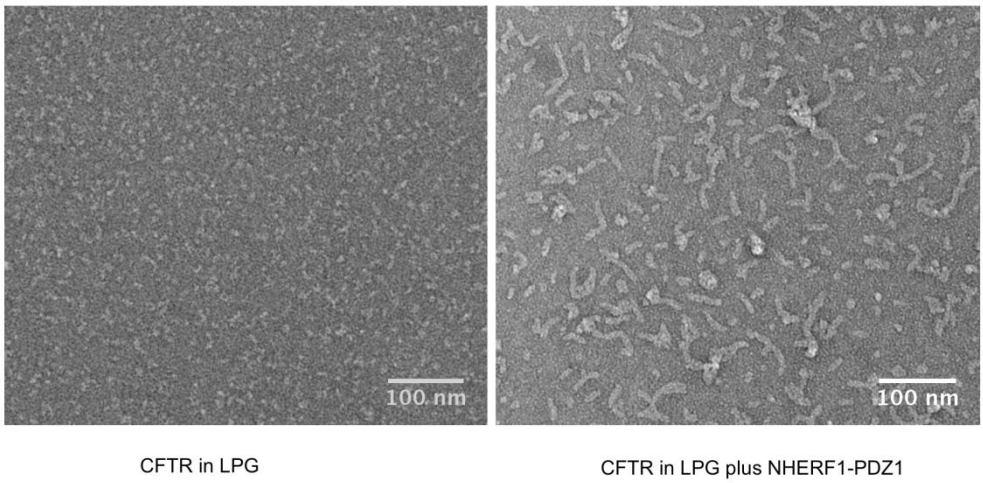

Figure 7. Electron micrographs of negatively stained CFTR particles purified in LPG (left) and after addition of NHERF1-PDZ1 domain (right). Addition of the domain induces a change in the morphology of the particles which form short strings probably composed of 2–10 CFTR complexes.

Although there is no experimental data on the binding site for glutathione in CFTR, a recent structure of a mitochondrial glutathione ABC transporter (Atm1) has revealed its substrate tightly bound to a site formed by 7 polar residues on the cytoplasmic ends of transmembrane helices 4,5 and 6 of one of the polypeptides forming the homodimeric transporter [45]. A comparison of amino acid residues found in the same positions in human ABCC transporter sequences (Supplementary Figures 8 and 9) shows some conservation in 6 of the 7 glutathione-binding residues in their TMD2 regions but no evidence for similar conservation in the TMD1 regions. This is not only the case for CFTR, but also for ABCC1, the archetypal glutathione-conjugate transporter in the family. Figure 8 shows residues in TMD2 that could form a glutathione binding site using a model of CFTR based on the Atm1 structure.

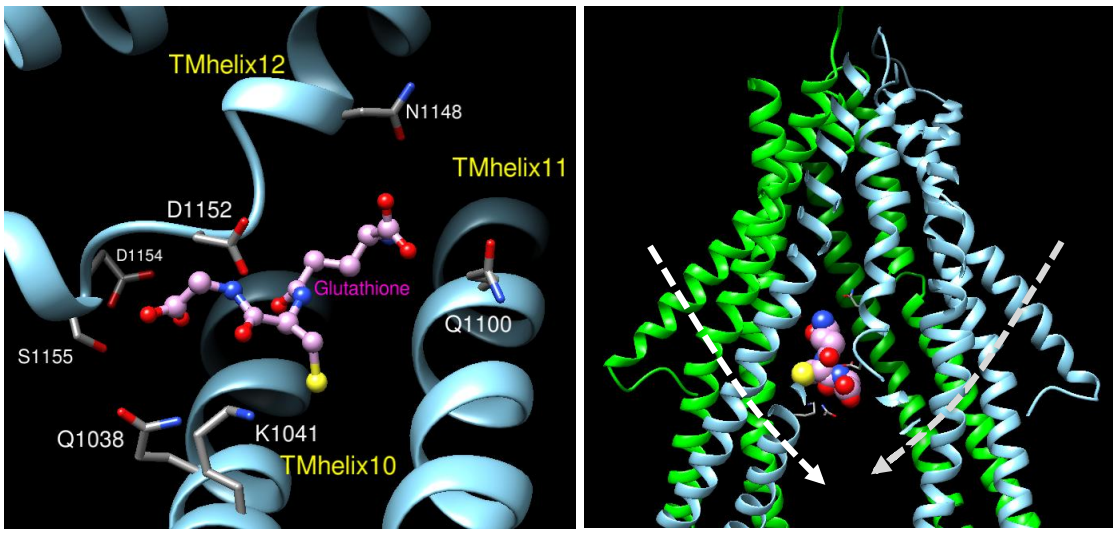

Figure 8. Homology model of CFTR based on the Atm1 structure showing a putative glutathione binding site formed by residues in transmembrane domain 2 (left panel). Conserved or conservatively replaced residues in TM helices 10–12 of CFTR that form the glutathione binding site in Atm1 are indicated. Right hand panel shows the global location of the predicted site in the TMDs. Glutathione bound in this position could impede the closure of the TMDs via prevention of scissoring movement (arrows) of the "swinging arm" formed by TM helices 10 and 11 (blue ribbons to the left). Formation of the NBD heterodimer needed for ATPase activity will thence be prevented.

Although the details shown in Figure 8 must be treated with a suitable degree of scepticism, it is interesting that alanine scanning mutagenesis of CFTR transmembrane helix 12 from residues 1147–1152 suggests a lack of helical structure, similar to the Atm1 structure [78]. Moreover, glutathione binding at this site in an inward-facing configuration of the CFTR structure would tend to block the rotation of transmembrane helices 10 and 11, needed to bring the NBDs into the catalytically-active heterodimer state (Figure 6, right panel, arrows). Glutathione in this hypothesis could prevent NBD1-NBD2 dimerisation and ATP hydrolysis, hence could prolong channel open times [73].

CF-causing mutations (http://www.genet.sickkids.on.ca/cftr/Home.html) have been documented and missense mutations cluster around the site shown in Figure 6. For example, D1152 when mutated to Histidine results in CF, whilst mutation of D1154 to either tyrosine or glycine results in a mild disease phenotype. In contrast, mutation of Q1100 to P in helix 11 and N1148 to lysine in helix 12 both result in severe disease. Further work is needed in order to establish whether these mutations will affect the ATPase activity of CFTR or influence the modulation of the activity by glutathione. The work here also points to a possible mechanism by which NHERF1 can regulate the function CFTR by stabilising it in an inward-facing state that presumably lacks ATPase activity. Separate studies by NMR have shown that the isolated C-terminal peptide can interact with the regulatory region of CFTR which might also provide a mechanism by which NHERF1 could influence the activity, localisation and maturation of CFTR [79].

5. Conclusion

Here we have shown that purified CFTR can adopt an inward-facing conformation when in the presence of NHERF1-PDZ1 domain. This conformation was predicted to exist for CFTR but had not been observed previously, even in the absence of nucleotide. The inward-facing conformation of CFTR could expose a binding site for glutathione, as predicted from homology modeling of the protein using the recent structure of a glutathione transporter. We find that glutathione can act as an inhibitor of the ATPase activity of CFTR. As ATP hydrolysis is thought to require the close association of the NBDs, a hypothesis where glutathione prevents the formation of such a configuration can be proposed and will be tested in future work.

Acknowlegements

The authors wish to thank the Cystic Fibrosis Foundation (CFF), the UK Cystic Fibrosis Trust, and the UK bbsrc for financial support. NC was a recipient of a bbsrc PhD studentship whilst AAZ was supported by the Saudi Educational Bureau. We also acknowledge colleagues in the CFF-funded CFTR 3D structure consortium for useful advice, discussions and providing reagents, in particular the codon-optimised chicken CFTR construct. We acknowledge the staff of the electron microscopy facility at the University of Manchester. Production of CFTR in mammalian cells in the Riordan laboratory was supported by NIH grants RO1-DK051619, RO1-DK051870 and PO1-HL110873.

Conflict of Interests

The authors declare no conflict of interests.

References

1. Cutting GR (2005) Modifier genetics: cystic fibrosis. *Annu Rev Genomics Hum Genet* 6: 237–260.
2. Higgins CF (1992) ABC transporters: from microorganisms to man. *Annu Rev Cell Biol* 8: 67–113.
3. Riordan JR, Rommens JM, Kerem B, et al. (1989) Identification of the cystic fibrosis gene: cloning and characterization of complementary DNA. *Science* 245: 1066–1073.
4. Gray MA, Winpenny JP, Verdon B, et al. (1995) Chloride channels and cystic fibrosis of the pancreas. *Biosci Rep* 15: 531–541.
5. McCarty NA (2000) Permeation through the CFTR chloride channel. *J Exp Biol* 203: 1947–1962.
6. Vankeerberghen A, Cuppens H, Cassiman JJ (2002) The cystic fibrosis transmembrane conductance regulator: an intriguing protein with pleiotropic functions. *J Cyst Fibros* 1: 13–29.
7. Riordan JR (2008) CFTR function and prospects for therapy. *Annu Rev Biochem* 77: 701–726.
8. Loo MA, Jensen TJ, Cui L, et al. (1998) Perturbation of Hsp90 interaction with nascent CFTR prevents its maturation and accelerates its degradation by the proteasome. *EMBO J* 17: 6879–6887.

9. Lukacs GL, Chang XB, Bear C, et al. (1993) The delta F508 mutation decreases the stability of cystic fibrosis transmembrane conductance regulator in the plasma membrane. Determination of functional half-lives on transfected cells. *J Biol Chem* 268: 21592–21598.
10. Lukacs GL, Segal G, Kartner N, et al. (1997) Constitutive internalization of cystic fibrosis transmembrane conductance regulator occurs via clathrin-dependent endocytosis and is regulated by protein phosphorylation. *Biochem J* 328 (Pt 2): 353–361.
11. O'Ryan L, Rimington T, Cant N, et al. (2012) Expression and purification of the cystic fibrosis transmembrane conductance regulator protein in Saccharomyces cerevisiae. *J Vis Exp*.
12. Huang P, Liu Q, Scarborough GA (1998) Lysophosphatidylglycerol: a novel effective detergent for solubilizing and purifying the cystic fibrosis transmembrane conductance regulator. *Anal Biochem* 259: 89–97.
13. Huang P, Stroffekova K, Cuppoletti J, et al. (1996) Functional expression of the cystic fibrosis transmembrane conductance regulator in yeast. *Biochim Biophys Acta* 1281: 80–90.
14. Ketchum CJ, Rajendrakumar GV, Maloney PC (2004) Characterization of the adenosinetriphosphatase and transport activities of purified cystic fibrosis transmembrane conductance regulator. *Biochemistry* 43: 1045–1053.
15. Krueger-Koplin RD, Sorgen PL, Krueger-Koplin ST, et al. (2004) An evaluation of detergents for NMR structural studies of membrane proteins. *J Biomol NMR* 28: 43–57.
16. Yang Z, Wang C, Zhou Q, et al. (2014) Membrane protein stability can be compromised by detergent interactions with the extramembranous soluble domains. *Protein Sci Public Protein Soci* 23: 769–789.
17. Matar-Merheb R, Rhimi M, Leydier A, et al. (2011) Structuring detergents for extracting and stabilizing functional membrane proteins. *PloS one* 6: e18036.
18. Galian C, Manon F, Dezi M, et al. (2011) Optimized purification of a heterodimeric ABC transporter in a highly stable form amenable to 2-D crystallization. *PloS one* 6: e19677.
19. Vinothkumar KR, Henderson R (2010) Structures of membrane proteins. *Q Rev Biophys* 43: 65–158.
20. Guggino WB (2004) The cystic fibrosis transmembrane regulator forms macromolecular complexes with PDZ domain scaffold proteins. *Proc Am Thorac Soc* 1: 28–32.
21. Karthikeyan S, Leung T, Birrane G, et al. (2001) Crystal structure of the PDZ1 domain of human Na(+)/H(+) exchanger regulatory factor provides insights into the mechanism of carboxyl-terminal leucine recognition by class I PDZ domains. *J Mol Biol* 308: 963–973.
22. Karthikeyan S, Leung T, Ladias JA (2002) Structural determinants of the Na^+/H^+ exchanger regulatory factor interaction with the beta 2 adrenergic and platelet-derived growth factor receptors. *J Biol Chem* 277: 18973–18978.
23. Li C, Naren AP (2011) Analysis of CFTR interactome in the macromolecular complexes. *Methods Mol Biol* 741: 255–270.
24. Li C, Roy K, Dandridge K, et al. (2004) Molecular assembly of cystic fibrosis transmembrane conductance regulator in plasma membrane. *J Biol Chem* 279: 24673–24684.
25. Wang S, Yue H, Derin RB, et al. (2000) Accessory protein facilitated CFTR-CFTR interaction, a molecular mechanism to potentiate the chloride channel activity. *Cell* 103: 169–179.

26. Bozoky Z, Krzeminski M, Muhandiram R, et al. (2013) Regulatory R region of the CFTR chloride channel is a dynamic integrator of phospho-dependent intra- and intermolecular interactions. *Proc Natl Acad Sci U S A*.
27. Guerra L, Favia M, Fanelli T, et al. (2004) Stimulation of Xenopus P2Y1 receptor activates CFTR in A6 cells. *Pflugers Arch* 449: 66–75.
28. Bossard F, Robay A, Toumaniantz G, et al. (2007) NHE-RF1 protein rescues DeltaF508-CFTR function. *Am J Physiol Lung Cell Mol Physiol* 292: L1085–1094.
29. Zhang L, Aleksandrov LA, Riordan JR, et al. (2011) Domain location within the cystic fibrosis transmembrane conductance regulator protein investigated by electron microscopy and gold labelling. *Biochim Biophys Acta* 1808: 399–404.
30. Zhang L, Aleksandrov LA, Zhao ZF, et al. (2009) Architecture of the cystic fibrosis transmembrane conductance regulator protein and structural changes associated with phosphorylation and nucleotide binding. *J Struct Biol* 167: 242–251.
31. Rosenberg MF, O'Ryan LP, Hughes G, et al. (2011) The cystic fibrosis transmembrane conductance regulator (CFTR): three-dimensional structure and localization of a channel gate. *J Biol Chem* 286: 42647–42654.
32. Dawson RJ, Locher KP (2006) Structure of a bacterial multidrug ABC transporter. *Nature* 443: 180–185.
33. Ward A, Reyes CL, Yu J, et al. (2007) Flexibility in the ABC transporter MsbA: Alternating access with a twist. *Proc Natl Acad Sci U S A* 104: 19005–19010.
34. Hildebrandt E, Zhang Q, Cant N, et al. (2014) A survey of detergents for the purification of stable, active human cystic fibrosis transmembrane conductance regulator (CFTR). *Biochim Biophys Acta* 1838: 2825–2837.
35. Al-Zahrani A (2014) Structural biology of Cystic Fibrosis Transmembrane Conductance Regulator, an ATP-binding cassette protein of medical importance. PhD Thesis, *University of Manchester*.
36. Pollock N, Cant N, Rimington T, et al. (2014) Purification of the cystic fibrosis transmembrane conductance regulator protein expressed in Saccharomyces cerevisiae. *J Vis Exp: JoVE*.
37. Chifflet S, Torriglia A, Chiesa R, et al. (1988) A method for the determination of inorganic-phosphate in the presence of labile organic phosphate and high-concentrations of protein-application to lens ATPases. *Anal Biochem* 168: 1–4.
38. Rothnie A, Theron D, Soceneantu L, et al. (2001) The importance of cholesterol in maintenance of P-glycoprotein activity and its membrane perturbing influence. *Eur Biophys J Biophys Lett* 30: 430–442.
39. Cant N, Pollock N, Rimington T, et al. (2014) Purification of the Cystic Fibrosis Transmembrane Conductance Regulator Protein Expressed in Saccharomyces cerevisiae. *J Vis Exp* 87.
40. Schultz BD, Bridges RJ, Frizzell RA (1996) Lack of conventional ATPase properties in CFTR chloride channel gating. *J Membr Biol* 151: 63–75.
41. Ludtke SJ, Baldwin PR, Chiu W (1999) EMAN: semiautomated software for high-resolution single-particle reconstructions. *J Struct Biol* 128: 82–97.

42. Zhang L, Aleksandrov LA, Riordan JR, et al. (2011) Domain location within the cystic fibrosis transmembrane conductance regulator protein investigated by electron microscopy and gold labelling. *Biochim Biophys Acta* 1808: 399–404.
43. Zhang L, Aleksandrov LA, Zhao Z, et al. (2009) Architecture of the cystic fibrosis transmembrane conductance regulator protein and structural changes associated with phosphorylation and nucleotide binding. *J Struct Biol*.
44. Henderson R, Sali A, Baker ML, et al. (2012) Outcome of the first electron microscopy validation task force meeting. *Structure* 20: 205–214.
45. Srinivasan V, Pierik AJ, Lill R (2014) Crystal structures of nucleotide-free and glutathione-bound mitochondrial ABC transporter Atm1. *Science* 343: 1137–1140.
46. Claude JB, Suhre K, Notredame C, et al. (2004) CaspR: a web server for automated molecular replacement using homology modelling. *Nucleic Acids Res* 32: W606–609.
47. Eswar N, Webb B, Marti-Renom MA, et al. (2007) Comparative protein structure modeling using MODELLER. *Current protocols in protein science/editorial board, John E Coligan* Chapter 2: Unit 2 9.
48. Laskowski RA, Rullmannn JA, MacArthur MW, et al. (1996) AQUA and PROCHECK-NMR: programs for checking the quality of protein structures solved by NMR. *J Biomol NMR* 8: 477–486.
49. Yang Z, Lasker K, Schneidman-Duhovny D, et al. (2012) UCSF Chimera, MODELLER, and IMP: an integrated modeling system. *J Struct Biol* 179: 269–278.
50. Zhang L, Aleksandrov LA, Riordan JR, et al. (2010) Domain location within the cystic fibrosis transmembrane conductance regulator protein investigated by electron microscopy and gold labelling. *Biochim Biophys Acta*.
51. Zhang L, Aleksandrov LA, Zhao Z, et al. (2009) Architecture of the cystic fibrosis transmembrane conductance regulator protein and structural changes associated with phosphorylation and nucleotide binding. *J Struct Biol* 167: 242–251.
52. Eckford PD, Li C, Ramjeesingh M, et al. (2012) Cystic fibrosis transmembrane conductance regulator (CFTR) potentiator VX-770 (ivacaftor) opens the defective channel gate of mutant CFTR in a phosphorylation-dependent but ATP-independent manner. *J Biol Chem* 287: 36639–36649.
53. Venerando A, Franchin C, Cant N, et al. (2013) Detection of phospho-sites generated by protein kinase CK2 in CFTR: mechanistic aspects of Thr1471 phosphorylation. *PloS one* 8: e74232.
54. Kogan I, Ramjeesingh M, Huan LJ, et al. (2001) Perturbation of the pore of the cystic fibrosis transmembrane conductance regulator (CFTR) inhibits its atpase activity. *J Biol Chem* 276: 11575–11581.
55. Aleksandrov AA, Kota P, Cui L, et al. (2012) Allosteric modulation balances thermodynamic stability and restores function of ΔF508 CFTR. *J Mol Biol* 419: 41–60.
56. Alexandrov AI, Mileni M, Chien EY, et al. (2008) Microscale fluorescent thermal stability assay for membrane proteins. *Structure* 16: 351–359.
57. Lysko KA, Carlson R, Taverna R, et al. (1981) Protein involvement in structural transition of erythrocyte ghosts. Use of thermal gel analysis to detect protein aggregation. *Biochemistry* 20: 5570–5576.

58. Soler G, Mattingly JR, Martinez-Carrion M (1984) Effects of heating on the ion-gating function and structural domains of the acetylcholine receptor. *Biochemistry* 23: 4630–4636.
59. Al Zahrani A (2014) PhD Thesis, University of Manchester.
60. Karthikeyan S, Leung T, Birrane G, et al. (2001) Crystal structure of the PDZ1 domain of human Na(+)/H(+) exchanger regulatory factor provides insights into the mechanism of carboxyl-terminal leucine recognition by class I PDZ domains. *J Mol Biol* 308: 963–973.
61. Krissinel E, Henrick K (2007) Inference of macromolecular assemblies from crystalline state. *J Mol Biol* 372: 774–797.
62. Karthikeyan S, Leung T, Ladias JA (2002) Structural determinants of the Na^+/H^+ exchanger regulatory factor interaction with the beta 2 adrenergic and platelet-derived growth factor receptors. *J Biol Chem* 277: 18973–18978.
63. Karthikeyan S, Leung T, Ladias JA (2001) Structural basis of the Na^+/H^+ exchanger regulatory factor PDZ1 interaction with the carboxyl-terminal region of the cystic fibrosis transmembrane conductance regulator. *J Biol Chem* 276: 19683–19686.
64. Zhang L, Aleksandrov LA, Zhao Z, et al. (2009) Architecture of the cystic fibrosis transmembrane conductance regulator protein and structural changes associated with phosphorylation and nucleotide binding. *J Struct Biol* 167: 242–251.
65. Gadsby DC, Vergani P, Csanady L (2006) The ABC protein turned chloride channel whose failure causes cystic fibrosis. *Nature* 440: 477-483.
66. Ma T, Thiagarajah JR, Yang H, et al. (2002) Thiazolidinone CFTR inhibitor identified by high-throughput screening blocks cholera toxin-induced intestinal fluid secretion. *J Clin Invest* 110: 1651–1658.
67. Verkman AS (1990) Development and biological applications of chloride-sensitive fluorescent indicators. *Am J Physiol* 259: C375–388.
68. Wellhauser L, Kim Chiaw P, Pasyk S, et al. (2009) A small-molecule modulator interacts directly with deltaPhe508-CFTR to modify its ATPase activity and conformational stability. *Mol Pharmacol* 75: 1430–1438.
69. Laverty G, Anttila A, Carty J, et al. (2012) CFTR mediated chloride secretion in the avian renal proximal tubule. *Comp Biochem Physiol A Mol Integr Physiol* 161: 53–60.
70. Cole SP (2014) Targeting multidrug resistance protein 1 (MRP1, ABCC1): past, present, and future. *Ann Rev Pharmacol Toxicol* 54: 95–117.
71. Paumi CM, Chuk M, Snider J, et al. (2009) ABC transporters in Saccharomyces cerevisiae and their interactors: new technology advances the biology of the ABCC (MRP) subfamily. *Microbiol Mol Biol Rev* 73: 577–593.
72. Maher P (2005) The effects of stress and aging on glutathione metabolism. *Ageing Res Rev* 4: 288–314.
73. Kogan I, Ramjeesingh M, Li C, et al. (2003) CFTR directly mediates nucleotide-regulated glutathione flux. *Embo J* 22: 1981–1989.
74. Roum JH, Buhl R, McElvaney NG, et al. (1993) Systemic deficiency of glutathione in cystic fibrosis. *J Appl Physiol* 75: 2419–2424.
75. Gao L, Kim KJ, Yankaskas JR, et al. (1999) Abnormal glutathione transport in cystic fibrosis airway epithelia. *Am J Physiol* 277: L113–118.

76. Marson FA, Bertuzzo CS, Ribeiro AF, et al. (2014) Polymorphisms in the glutathione pathway modulate cystic fibrosis severity: a cross-sectional study. *BMC Med Genet* 15: 27.
77. Rubera I, Duranton C, Melis N, et al. (2013) Role of CFTR in oxidative stress and suicidal death of renal cells during cisplatin-induced nephrotoxicity. *Cell Death Disease* 4: e817.
78. Cui G, Song B, Turki HW, et al. (2012) Differential contribution of TM6 and TM12 to the pore of CFTR identified by three sulfonylurea-based blockers. *Pflugers Arch: Eur J Physiol* 463: 405–418.
79. Bozoky Z, Krzeminski M, Muhandiram R, et al. (2013) Regulatory R region of the CFTR chloride channel is a dynamic integrator of phospho-dependent intra- and intermolecular interactions. *Proc Natl Acad Sci U S A* 110: E4427–4436.